

Supporting Information

Periasamy et al. 10.1073/pnas.1115006109

SI Methods

Bacterial Strains and Growth Conditions. The clinical community-associated methicillin-resistant *S. aureus* isolates USA300 (clone LAC) (1) or USA400 (clone MW2) (2, 3) and isogenic *psm* and *agr* deletion mutants (4, 5) were used for all experiments. Of note, in Δhld strains, translation of *hld* is abolished by a single base mutation of the start codon, which allows for maintained function of RNAIII. Plasmids for expression of phenol-soluble modulins (PSM) peptides in the *psm* triple mutant were produced by cloning the *psm* α , *psm* β , or *hld* genes into plasmid pTX15 (6) through the BamH1/Mlu1 sites. Promoter-*egfp* fusion constructs were produced by cloning the respective promoter fragments and a *Staphylococcus* codon use-optimized *egfp* gene into plasmid pRB473, which was previously described for the *psm* β promoter of *S. epidermidis* (7). Oligonucleotides used for amplification are shown in Table S1.

Cells were grown in tryptic soy broth (TSB) supplemented with 0.5% glucose except for the xylose induction experiments, in which glucose-free TSB was used with or without 0.5% xylose. When appropriate, tetracycline (12.5 $\mu\text{g}/\text{mL}$) or chloramphenicol (10 $\mu\text{g}/\text{mL}$) was added.

1. CDC (2003) Outbreaks of community-associated methicillin-resistant *Staphylococcus aureus* skin infections—Los Angeles County, California, 2002–2003. *MMWR Morb Mortal Wkly Rep* 52:88.
2. CDC (1999) From the Centers for Disease Control and Prevention. Four pediatric deaths from community-acquired methicillin-resistant *Staphylococcus aureus*—Minnesota and North Dakota, 1997–1999. *JAMA* 282:1123–1125.
3. Baba T, et al. (2002) Genome and virulence determinants of high virulence community-acquired MRSA. *Lancet* 359:1819–1827.
4. Wang R, et al. (2007) Identification of novel cytolytic peptides as key virulence determinants for community-associated MRSA. *Nat Med* 13:1510–1514.
5. Joo HS, Cheung GY, Otto M (2011) Antimicrobial activity of community-associated methicillin-resistant *Staphylococcus aureus* is caused by phenol-soluble modulins derivatives. *J Biol Chem* 286:8933–8940.

Biofilm Microtiter Plate Assays. For the analysis of the impact of synthetic PSMs on biofilm formation, microtiter plate assays were performed as previously described (4). Briefly, each microtiter well was inoculated with the LAC *agr* mutant from a preculture grown overnight (1:100 volume), PSMs were added, and the plate was incubated for 24 h at 37 °C. Then, biofilms were washed gently with water and stained using safranin.

PSM Analysis. PSM concentrations in planktonic cultures and flow cell effluents were measured using reversed-phase HPLC/MS as previously described (4). Flow cell effluents were concentrated using precipitation with ice-cold trichloroacetic acid (1/5 volume) and redissolved in 8 M urea for analysis.

Computer Analysis of Confocal Laser-Scanning Microscopy Images. Total and average biovolumes were calculated using Imaris 7.2 software. Mean thickness and roughness coefficients were calculated using Comstat software (8).

Statistics. Statistical analysis was performed using Graph Pad Prism Version 5 with two-tailed unpaired *t* tests (two groups) unless noted otherwise.

6. Peschel A, Ottenwalder B, Gotz F (1996) Inducible production and cellular location of the epidermin biosynthetic enzyme EpiB using an improved staphylococcal expression system. *FEMS Microbiol Lett* 137:279–284.
7. Wang R, et al. (2011) *Staphylococcus epidermidis* surfactant peptides promote biofilm maturation and dissemination of biofilm-associated infection in mice. *J Clin Invest* 121: 238–248.
8. Heydorn A, et al. (2000) Quantification of biofilm structures by the novel computer program COMSTAT. *Microbiology* 146:2395–2407.

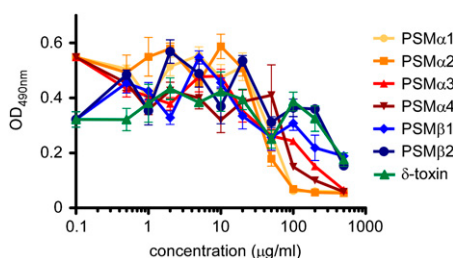


Fig. S1. Impact of synthetic PSMs on static biofilm formation. Synthetic (*N*-formylated) PSMs at different concentrations were added at the time of inoculation from precultures to cultures of *S. aureus* LAC Δagr . Biofilms were grown in TSB/0.5% glucose in 96-well microtiter plates for 24 h. Then, biofilm formation was analyzed by safranin staining and measuring OD_{490} . Values represent means \pm SEM of four replicate wells.

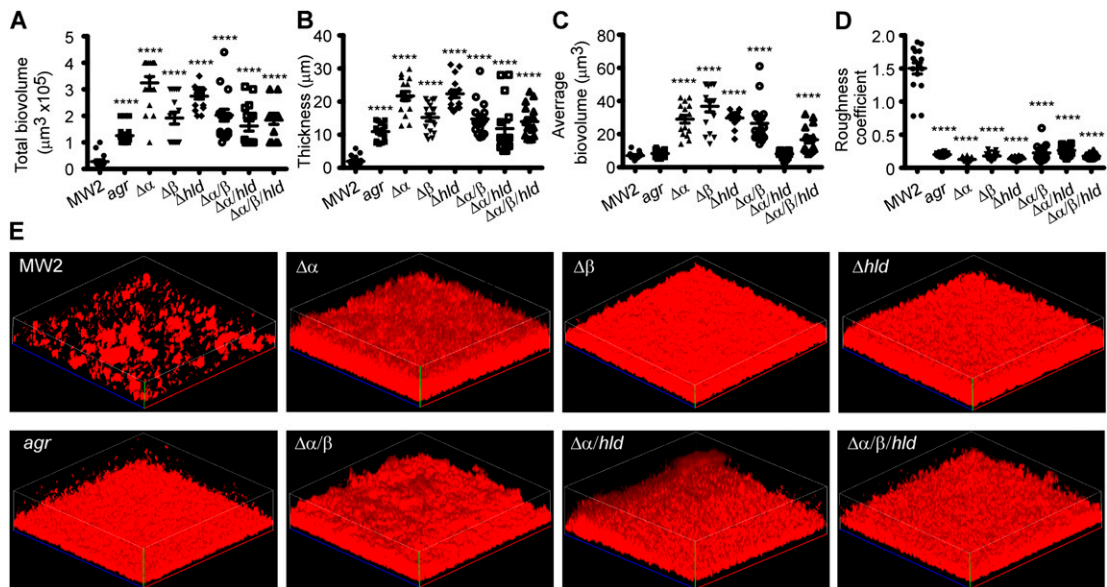


Fig. S2. Impact of PSMs and Agr on the structuring of static *S. aureus* MW2 biofilms. Static biofilms were grown in eight-well chambered coverglass plates for 48 h. (A–D) Biofilm parameters were measured in 16 randomly chosen biofilm confocal laser-scanning microscopy (CLSM) images of the same extension. Horizontal bars depict the mean. Statistical analysis is by *t* tests vs. the corresponding values of the WT samples, which were grown and measured separately for every mutant comparison. Only one WT analysis is shown for brevity; however, statistical analysis was performed vs. the corresponding WT samples grown in parallel, which were very similar in all cases. **** $P < 0.0001$. Values for 24-h biofilms were also measured, and differences were similar. (E) Example 48-h CLSM biofilm images. Extensions and scales are the same in every image (total x extension, 230 μm ; total y extension, 230 μm).

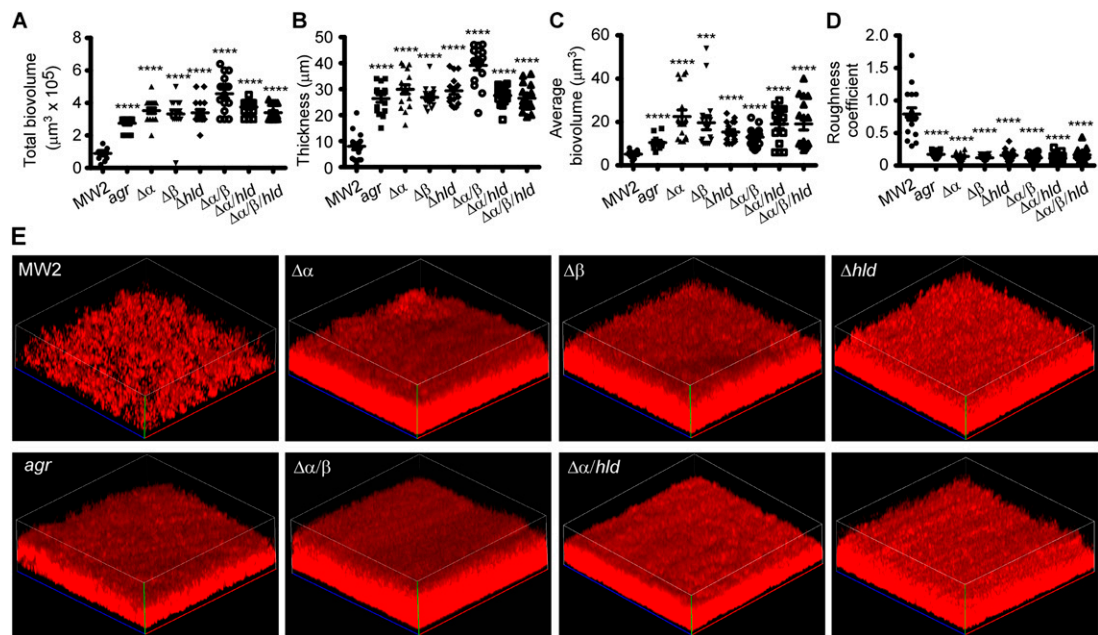


Fig. S3. Impact of PSMs and Agr on the structuring of dynamic (flow cell) *S. aureus* MW2 biofilms. Dynamic (flow cell) biofilms were grown for 72 h. (A–D) Biofilm parameters were measured at 72 h in 16 randomly chosen biofilm CLSM images of the same extension. Horizontal bars depict the mean. Statistical analysis is by *t* tests vs. the corresponding values of the WT samples, which were grown and measured separately for every mutant comparison. Only one WT analysis is shown for brevity; however, statistical analysis was performed vs. the corresponding WT samples grown in parallel, which were very similar in all cases. *** $P < 0.001$; **** $P < 0.0001$. (E) Example 48-h CLSM biofilm images. Extensions and scales are the same in every image (total x extension, 230 μm ; total y extension, 230 μm).

